COMPARING THE MELANIN-CONCENTRATING HORMONE -1 RECEPTOR EXPRESSION IN THE BRAINS OF MICE AND RATS

by

SIDNEY CLAYBORN WILLIAMS III

Presented to the Faculty of the Graduate School of

The University of Texas at Arlington in Partial Fulfillment

of the Requirements

for the Degree of

MASTER OF SCIENCE IN BIOLOGY

THE UNIVERSITY OF TEXAS AT ARLINGTON

May 2007

ACKNOWLEDGEMENTS

First of all, I would like to thank my wife, Lisa for her constant encouragement, boundless energy and her ability to keep me motivated when I felt overwhelmed. Also, I could not have accomplished my goals without the inexhaustible support and love from my parents for which I will always be truly thankful. I would like to thank Dr. Howard Arnott for being my mentor and a superb teacher over the years as well as introducing me to scientific research and allowing me to pursue my own interest. I would also like to thank Dr. Perry Fuchs and Dr. James Robinson for kindly sitting on my committee and giving me invaluable advice. I have to thank Dr. Masashi Yanagisawa for allowing me to pursue my Masters degree while working full time and letting me perform these experiments in his lab. A special thanks goes to Dr. Yuichi Ikeda for his excellent teaching in molecular biology and to Dr. Christopher Sinton for always finding the time to help me when I have questions about sleep research. Thanks to Dr. Joel Elmquist and Charlotte Lee for sharing their neurobiology expertise and histology techniques! A big thanks goes to the Howard Hughes Medical Institute for having a tuition reimbursement program that paid for this portion of my education. Last, but not least, I would like to thank Amber Skach for being so organized and for pursuing a graduate degree with me.

April 11, 2007

ABSTRACT

COMPARING THE MELANIN-CONCENTRATING HORMONE -1 RECEPTOR EXPRESSION IN THE BRAINS OF MICE AND RATS

Publication No. _____

Sidney Clayborn Williams III, M.S.

The University of Texas at Arlington, 2007

Supervising Professor: Dr. Howard Arnott

The melanin-concentrating hormone (MCH) family of neuropeptides is believed to be important in controlling certain feeding behaviors. This family consists of one ligand, melanin-concentrating hormone (MCH), and two receptors, melanin-concentrating-1 receptor (MCH-1R) and melanin-concentrating-2 receptor (MCH-2R), of which only MCH-1R is expressed in rodents. Recently, the distribution of MCH-1R in rat brains was published revealing that it is expressed throughout the rat brain in a complex and widespread manner. Moreover, mice lacking MCH and MCH-1R have been generated and have been found to be leaner and more active than their wild-type littermates. Consequently, MCH-1R has become a possible site for pharmacological interaction to control obesity. Many of these experiments are being performed utilizing

mice however, the areas expressing MCH-1R in the mouse brain still remain unknown. Therefore, *in situ* hybridization was performed in both mouse and rat brain samples to elucidate the MCH-1R mRNA expression in the mouse and to compare these results with the expression in the rat. This comparison study revealed that most of the positive nuclei evaluated were represented in both rodent models and that these areas displayed similar expression intensities. However, a subset of nuclei was found to display a different MCH-1R expression between these two rodent species. These expression differences reside in brain areas important in reward, motivation, movement, visualization, vigilance, and learning, and could possibly explain differences in feeding and foraging behaviors between mice and rats.

TABLE OF CONTENTS

LIST OF ILLUSTRATIONS

Figure Page

LIST OF TABLES

CHAPTER 1

INTRODUCTION

Melanin concentrating hormone (MCH) is a highly conserved 19 amino acid neuropeptide found in vertebrates, including fish, rodents and humans. MCH was first isolated from the pituitary of salmon and was found to control the aggregation of the skin pigment melanin (Kawauchi et al., 1983); hence the nomenclature of the neuropeptide. It was subsequently isolated from rat hypothalamus (Vaughan et al., 1989), and this finding sparked intense research on MCH in mammals. Immunohistochemical studies in the rat have shown that MCH is produced uniquely in the hypothalamus with the majority of the cell bodies located in the perifornical area of the lateral hypothalamus (LH) and within the zona inserta (Bittencourt et al., 1992). The latter study also revealed that MCH neurons send widespread projections throughout the forebrain including the olfactory bulb, cortex, hippocampus, and amygdaloid complex, as well as to hindbrain structures, including the pontine formation and medulla oblongata (Bittencourt et al., 1992). This extensive innervation suggests that MCH controls or influences many neuronal functions.

Qu et al. (1996) noted that direct intracerebroventricular (ICV) injection of MCH in mice increased food intake. These authors also reported that fasting mice showed an increase of MCH mRNA levels in the LH. Furthermore, MCH null mice are lean, hypophagic and have higher metabolic rates than their wild-type littermates

(Shimada et al., 1998). Conversely, transgenic mice over-expressing MCH are hyperphagic and mildly obese (Ludwig et al., 2001). These findings thus provided a possible explanation for an early study in which neurons were ablated in the LH area, resulting in hypophagia and excessive weight loss (Teitelbausm et al., 1969). More recent studies have shown that MCH is responsive to the fat-related hormone, leptin (Ito M., 2003). The neuropeptide also stimulates the release of the orexigenic NPY and agouti-related peptides, but inhibits the anorexic alpha-melanocyte-stimulating hormone (αMSH) and cocaine- and amphetamine-related (CART) neuropeptides (Abbott et al., 2003). Taken together, these results clearly indicate that MCH plays a role in feeding behavior and metabolism.

Several research groups identified the endogenous receptor for MCH as the orphan G-protein coupled receptor SLC-1, also called GPR-24, and named the receptor MCH-R, later MCH-1R (Bachner et al., 1999; Chambers et al., 1999; Lembo et al., 1999; Saito et al., 1999; Shimomura et al., 1999). SLC-1 was first isolated and described by Kolakowski et al. (1996) and was shown to have a 40% homology to the human somatostatin receptor. Subsequently, a second G-protein coupled receptor (MCH-2R) specific to MCH was identified but was found not to be expressed in rodents (Hill et al., 2001; Sailer et al., 2001; Tan et al., 2002; Wang et al., 2001). To elucidate the functions of MCH-1R, transgenic mice lacking the receptor were generated. These MCH-1R null (i.e., MCH-1R$^{-/-}$) mice are lean, hyperphagic and hyperactive during the dark phase of the light-dark cycle (Chen et al., 2002; Marsh et al., 2002). Having normal body weight, the leanness in the MCH-1R null mouse is a consequence of

reduced fat pad volume and higher energy expenditure due to hyperactivity (Chen et al., 2002; Marsh et al., 2002). This hyperactivity offset the hyperphagia and increased the resistance of the mice to diet-induced obesity (Chen et al., 2002; Marsh et al., 2002). These findings correlated well with results in the MCH ligand knockout mouse and indicated that the MCH-1R could be a potential target for pharmacological manipulation to regulate food intake. Indeed, chronic infusion of an MCH-1R antagonist in rats reduced food intake, and decreased body weight and adiposity without a reduction in lean mass (Shearman et al., 2003). Additionally, infusion of an MCH-1R antagonist in diet-induced obese mice not only dramatically decreased both food intake and body weight, but also reversed obesity related problems including high levels of cholesterol, insulin, glycerides, and leptin (Mashiko et al., 2005). Interestingly, MCH-1R antagonists also have antidepressant and anxiolytic effects (Borowsky et al., 2003).

The MCH-1R has a widespread expression pattern throughout the rat brain. Strong MCH-1R mRNA expression in the olfactory nuclei and piriform complex has been shown, which is associated with odor detection; in the hippocampus and amygdala, which have been linked with learning and memory; and in the locus coeruleus, a canonical arousal center (Kolakowski et al., 1996; Chambers et al., 1999; Lembo et al., 1999; Saito et al., 1999; Civelli et al., 2001). Marked expression was also observed in the accumbens shell, which is linked with motivated behavior and feeding (Kolakowski et al., 1996; Chambers et al., 1999; Lembo et al., 1999; Saito et al., 1999; Civelli et al., 2001). Other feeding-related areas of the brain including the ventromedial hypothalamic nucleus, the arcuate nucleus and zona incerta showed only moderate

expression (Kolakowski et al., 1996; Chambers et al., 1999; Lembo et al., 1999; Saito et al., 1999; Civelli et al., 2001). These areas, as well as others expressing MCH-1R, correlate well with immunohistochemical determinations of the MCH projections (Bittencourt et al., 1992; Civelli et al., 2001)

Most of the studies describing the expression pattern of MCH-1R have been preformed on rat brain. Only one publication has been published that contains MCH-1R *in situ* hybridization results from mouse brain tissue and this study was designed to verify the absence of MCH-1R mRNA in a MCH-1R knockout mouse (Marsh et al., 2002). There is thus currently no information about the expression pattern of MCH-1R in mouse brain, which is the goal of the present study. We have used radioactive *in situ* hybridization techniques to describe the detailed expression pattern of MCH-1R in mouse brain and compare these results with those from rat brain.

CHAPTER 2

MATERIALS AND METHODS

2.1 Tissue Preparation

All animals used in this study were housed in the animal facility at UT Southwestern Medical Center in Dallas on a 12 hour on / 12 hour off light cycle with food and water freely available. All procedures followed protocols and guidelines that were approved by the University of Texas Southwestern Medical Center at Dallas Institutional Animal Care and Use Committee. Mice were anesthetized with a lethal 250µl I.P. injection of 250mg/kg ketamine and 25mg/kg xylazine and were allowed to reach a state of non-responsiveness to a foot or tail pinch. Animals were then transcardially perfused using approximately 20ml of diethyl-pyrocarbonate (DEPC) treated heparinized (10units/ml of heparin) saline followed by 50ml of 4% paraformaldehyde /DEPC Phosphate buffered saline (4% PFA) pH. 7.4. The brains were quickly removed and allowed to fix in the 4% PFA solution overnight on a shaker at 4˚C. The fixative was decanted and replaced with DEPC treated 30% Sucrose and the brains were allowed to cyro-protect for 48 hours or until they had sunk to the bottom of the 50ml conical tube. Using powdered dry ice, the brains were then frozen vertically onto a freezing platform (Brain Research Laboratories, Waban, MA) and sectioned coronally at a thickness of 30µm with a Leica 2000R sliding microtome (Leica Microsystems, Bannockburn, IL). Sections were transferred to DEPC PBS in a

one to four ratio allowing multiple experiments to be performed on the same brain. If the sections were not used immediately, they were stored at -20˚C in 1ml cryogenic vials containing an anti-freeze media (50% DEPC PBS, 30% ethylene glycol, 20% glycerol).

2.2 Probe Construction

Three mRNA probes were constructed representing the whole coding region for MCH-1R. The oligonucleotide primer sequences were obtained by using the program GeneTx and are as follows:

Forward Sequence 1 (4-21)

5′-GAT CTG CAA GCC TCG TTG -3′

Reverse Sequence 1 (329-312)

5′-TGC CAG ACA CCA TTA CCC -3′

Forward Sequence 2 (392-412)

5′-CCT ACA TCE TGA CTG CTA TGG -3′

Reverse Sequence 2 (795-776)

5′−GAA GAC CAG ACA GAT CAT CAG -3′

Forward Sequence 3 (831-848)

5′−GAC CCA GTT GTC CAT CAG -3′

Reverse Sequence 3 (1062-1145)

5′−TCA GGT GCC TTT GCT TTC-3′

Polymerase chain reaction (PCR) was performed using these primers based on a full

mouse brain cDNA library. The resulting PCR products were purified using QIAquick (QIAGEN, Valencia, CA) and ligated into pGEM-T Easy Vectors plasmids (Promega, Madison, WI). These plasmids were transformed into JM109 competent cells and plated on LB agar plates containing x-gal reagent as well as ampicillin and incubated overnight at 37˚C. Individual white colonies were picked with sterilized wooden toothpicks and placed into LB broth media and again incubated overnight at 37˚C. A miniprep was performed to isolate the plasmids which were then sent to be sequenced. Selected plasmids were amplified and then isolated using a miniprep kit (QIAGEN, Valencia, CA). To obtain anti-sense probes, the plasmids were linearized using the restriction enzyme *SpeI* and *ApaI* for sense probes. *In vitro* transcription (IVT) was performed with the Ambion Maxi Script kit (Ambion, Austin, TX) utilizing T7 and Sp6 RNA polymerases for anti-sense and sense probes, respectively. To increase the specific activity of the radioactive probes, ^{35}S UTP and ^{35}S CTP (Amersham, Arlington Heights, IL) radionucleotides were both used in the IVT procedure. All of the unincorporated nucleotides were removed using G-50 spin columns (Roche, Indianapolis, IN) and the purified probes were stored at -80˚C until needed.

2.3 *In Situ* Hybridization

The following procedure was performed using RN'ase free techniques and with DEPC treated chemicals to help maintain the integrity of the sensitive mRNA inside the tissue samples. All chemical washes were performed in RN'ase free glass staining dishes for 5 minutes unless stated otherwise. Slides that were stored at -20˚C were allowed to reach room temperature and then placed in 30 count metal slide racks. The

tissues were dilapidated by immersing the racks twice in xylene for 10 minutes followed by three washes in 100% ethanol. The tissues were re-hydrated in a decreasing gradient of ethanol that was diluted with DEPC Saline (95%, 80%, 60%, 30%) followed by a wash in saline. Slides were transferred into upright plastic racks for microwave RNA retrieval. The upright racks were immersed in 1X Antigen Retrieval Citra pH 6.0 (Biogenex, San Ramon, CA) in a one-liter boiling dish making sure that all tissues were submerged. The boiling dish was placed into a microwave with the temperature probe positioned in the Citra solution and the slides were microwaved at a temperature of 100˚C for 10 minutes. Slides were allowed to cool to room temperature and transferred back to the metal racks to continue the pre-hybridization washes. The slides were washed twice in phosphate buffered saline (PBS), pH 7.4, fixed in 4% PFA, for 10 minutes, followed by two PBS washes. To further permeate the tissues, the slides were incubated in pronase E (20mg/ml pronase-E in 50 mm Tris-HCl, pH 8.0/5 mm EDTA, pH 8.0/DEPC-H_2O) for 7.5 minutes followed by a PBS wash. Then the slides were again placed into 4% PFA, rinsed twice in PBS and then acetylated with two washes of acetic anhydride (0.25% acetic anhydride/0.1m triethanolamine–HCl, pH 7.0). The slides were rinsed in 1X standard saline citrate buffer, pH 7.0, (1X SSC) followed by a 10-minute incubation in NEM (50 mm n-ethylmaleimide/1x SSC, pH 7.0). Finally, the sections were rinsed in PBS, then saline, and dehydrated by an increasing gradient of ethanol (30%, 60%, 80%, 95%, 100%X3). To dry the tissue totally, the racks were placed in a vacuum chamber for 2 hours.

Radioactive RNA probes and hybridization mixture (50% formamide, 0.6m

NaCl, 20 mm Tris-HCl, pH 8.0, 5 mm EDTA, pH 8.0, 10 mm NaPO4, pH 8.0, 10% dextran sulfate, 1X Denhardt's, 0.5 mg/ml tRNA) were removed from -80˚C storage and allowed to reach room temperature. To determine the amount of radioactivity that the riboprobes contained, 1µl of each probe was added to 5 ml of counting cocktail in glass scintillation vials and measured using a Beckman LS 6500 scintillation counter (Beckman Coulter, Inc., Fullerton, CA). These data were used to calculate the amount of probe needed per volume of hybridization mixture to obtain a final radioactivity of $7.5X10^3$ cpm/µl. Once the correct volume of probe was added to the hybridization mix, the combined mixture was vortexed and heated to 95˚C for 5 minutes and then cooled to 37˚C. Before the probe was applied onto the microscope slides, 1M DTT was added to the final hybridization mixture equaling 1% of the total hybridization volume. The slides were removed from the vacuum chamber and 150µl of the probe hybridization mixture was carefully applied directly to each corresponding slide making sure all the tissue was covered. Next, the slide was placed into a Nalgene hybridization box with 5X SSC/50% formamide saturated gel blot paper lining the bottom. To make sure the hybridization mixture did not dry or move off the tissue, a plastic coverslip was placed on top of each microscope slide. The box was then wrapped in clear wrap, the top securely set in place, and then placed in a 65˚C hybridization oven for 8 to 12 hours.

The slides were removed from the hybridization oven, their coverslips were manually removed with fine forceps, and they were placed in 25 count plastic vertical racks. Immediately, the racks were immersed in 5X SSC/10mM DTT at 55˚C for 40 minutes followed by a 30 minutes high stringency HS (2X SSC/50%

formamide/100mM DTT) buffer wash at 65˚C. Subsequently, the slides were washed three times in NTE (0.5M NaCl/10mM Tris-HCL, pH 8.0,/5mM EDTA, pH 8.0) at 37˚C for 10 minutes each. To rid the sections of all remaining unincorporated riboprobe, the slides were incubated in a NTE wash containing RN'ase-A (2µg/ml) for 30 minutes at 37˚C. This step was followed by a final NTE wash for 15 minutes at 37˚C. The slides were once again placed in the HS wash for 30 minutes followed by two 30 minute washes in 2X SSC/10mM DTT at 50˚ C and 1X SCC/ 10mM DTT at 55˚C. Finally the slides were rinsed in 0.1X SSC at 37˚C, dehydrated in graded ethanols (30%, 60%, 80%, 95%, 100%) and dried under vacuum.

2.4 Dark Room Procedures

The radioactive *in situ* slides were taped tissue side up onto the inside of a large autoradiographic cassette. Under safe light conditions, Kodak BioMax MR film was placed directly on top of the slides and the cassette was securely closed. The film was allowed to expose for 24 hours and then developed using an automatic developer. This procedure was repeated allowing the film to be exposed for 48 hours. Next, the slides were removed from the cassette, placed in grippets, and dipped in Ilford K.5 nuclear emulsion (Polysciences, Warrington, PA) that was pre-warmed to 42˚C in a water bath. Slides were allowed to dry vertically in a custom box under high humidity for 4 to 12 hours. After the slides had completely dried, they were carefully transferred to 25-count plastic microscope slide storage boxes with desiccant. The boxes were sealed with tape and wrapped twice with foil to prevent any light leaks. Finally, the boxes were placed at 4˚C for a specific exposure time determined from the autoradiographic

films, which is usually 1 to 4 weeks. Once the exposure time had was reached, the boxes were removed from the 4˚C storage and allowed to reach room temperature. The slides were then transferred to a metal 30-count metal rack, developed in D-19 (Eastman Kodak, Rochester, NY) at 15˚C for 2.5 minutes, rinsed quickly in water containing 1% glacial acetic acid, and then fixed in Kodak fixer for 5 minutes. Under running tap water, the slides were rinsed very well, counterstained in hematoxylin (Richard-Allen, Kalamazoo, MI), dehydrated in 100% ethanols, cleared in Xylenes, and coverslipped using a permanent mounting media.

2.4 Data Evaluation

The expression of MCH-1R mRNA in the mouse and rat brain was evaluated and qualitatively analyzed by utilizing autoradiographic films as well as developed microscope slides dipped in photographic emulsion. The autoradiographic films were scanned into Adobe Photoshop SC2 (San Jose, CA) utilizing the scanning software SilverFast Ai (Microtek, Carson, CA) controlling a Microtek ScanMaker i900 (Carson, CA) flatbed scanner at a resolution of 1000dpi to facilitate evaluation. The microscope slides were evaluated and photographed at low and high magnifications using both brightfield and darkfield lighting techniques. Low magnification images were captured using an Olympus SFZ stereo microscope outfitted with a darkfield condenser and an Optronics (Goleta, CA) digital camera which was controlled by NIH Image. A Nikon 80i microscope was used for high magnification image capture utilizing a Nikon DXM1200F digital camera and NIS Elements imaging software. Anatomical regions specifically expressing MCH-1R mRNA were identified by comparing slides

hybridized with sense and anti-sense radioactive probes. The nomenclature from the Paxinos and Franklin (2004) mouse brain atlas and the Paxinos and Watson (2005) rat brain atlas were used to correctly name these positive regions. The qualitative expression levels were measured by the relative intensity of the radioactive signal as well as the number of positive cells residing in the area of evaluation and was annotated as follows: + + + +, very strong expression, + + +, strong expression, + +, moderate expression, +, low expression, -, background or no expression, +/-, inconsistent expression, n/a, area not available for evaluation. Adobe Photoshop SC2 was used to clean darkfield images of any obvious dust, to adjust contrast and brightness, and to assemble and label all figures.

CHAPTER 3

RESULTS

Radioactive *in situ* hybridization for MCH-1R mRNA was performed using both mouse and rat frozen brain tissue sections. These sections represented the entire brain region from the olfactory and forebrain areas to the most caudal areas of the medulla. Hybridization with anti-sense probes revealed a complex and wide spread expression pattern within the rodent brains. Strong MCH-1R expression was observed in the olfactory, cerebral cortex, hippocampal, and basal areas as well as weak to moderate expression in the, amygdala, thalamus, and hypothalamic areas (Figs. 3.2, 3.3, 3.6, 3.7). Moderate signal was also found in the mid-brain and brain-stem structures including the pons and medulla oblongata areas (Figs 3.3, 3.4, 3.5, 3.7, 3.8). Conversely, no expression was observed when sections were hybridized with sense probe (Figure 3.1).

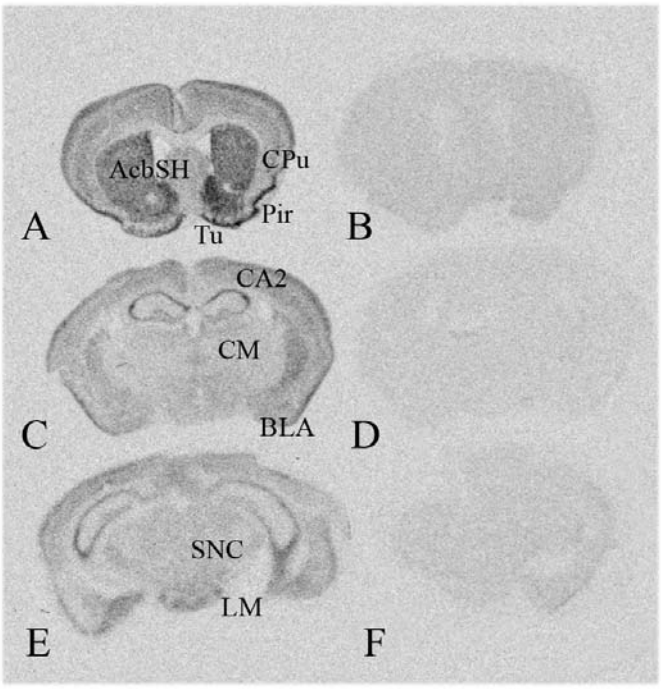

Figure 3.1: MCH-1R anti-sense and sense probe results
((A, C, E) anti-sense and (B, D, F) sense)
(Please see tables for an explanation of the abbreviations.)

3.1 Cerebral Cortex

MCH-1R mRNA was expressed throughout the entire length of the cerebral cortex in both rat and mice (Table 3.1). The signal was mostly concentrated in two layers of the cortex, layer II/III and V. The highest expression was observed in the piriform cortex followed by strong expression in the ventral, medial, and lateral orbital cortex, perirhinal cortex, and areas 1 and 2 of the cingulate cortex (Figs. 3.2A-F, 3.3G-L, 3.6A-F, 3.7G-K). Strong expression was also seen in the agranular and granular retrosplenial cortexes, prelimbic cortex, and in the secondary motor cortex (Figs. 3.2A-F, 3.3G-I, 3.6A-F, 3.7G,H). The dorsal and ventral agranular insular cortexes expressed only moderate signal in both mice and rats along with ectorhinal, frontal association,

and primary motor cortexes (Figs. 3.2A-F, 3.3G-I, 3.6A-F, 3.7G,H). Moderate signal was observed in the cingulum as well (Figs. 3.2C, 3.6C). The auditory, primary and secondary somatosensory, and the temporal association cortexes expressed moderate signal in the mouse but expressed weakly in the rat (Figs. 3.2C, 3.3L, 3.6E, 3.7J). Weak expression was observed in the dysgranular insular cortex in both species (Figs. 3.2C, 3.6B). The majority of areas expressing MCH-1R mRNA in the cerebral cortex displayed similar signal strengths between the mouse and rat brain samples. However, the claustrum and the dorsal endopiriform cortex (most rostral aspect) expressed moderate signal in the rat but no signal was observed in these areas in the mouse (Figs. 3.6D,E, 3.9A-C). Interestingly, MCH-1R begins to be weakly expressed in the dorsal endopiriform cortex in the midbrain region (Fig. 3.3J,K).

Table 3.1: Relative Expression Densities of MCH-1R in the Cerebral Cortex

	Mouse	Rat
Agranular insular cortex (AI)	+ + +	+ +
Agranular insular cortex, dorsal (AID)	+ +	+ +
Agranular insular cortex, ventral (AIV)	+ +	+ +
Auditory cortex, (Au)	+ +	+
Claustrum (Cl)	-	+ +
Cingulate cortex, area 1 (Cg1)	+ + +	+ + +
Cingulate cortex, area 2 (Cg2)	+ + +	+ + +
Cingulum (cg)	+ +	+ +
Dysgranular insular cortex, (DI)	+	+
Ectorhinal cortex, (Ect)	+ +	+ +
Endopiriform cortex, dorsal (DEn)	+/-	+ +
Frontal association cortex (FrA)	+ +	+ +
Motor cortex, primary, (M1)	+ +	+ +
Motor cortex, secondary (M2)	+ + +	+ + +
Orbital cortex, ventral (VO)	+ + +	+ + +
Orbital cortex, medial (MO)	+ + +	+ + +
Orbital cortex, lateral (LO)	+ + +	+ + +

Table 3.1: *Continued*

Perirhinal cortex (PRh)	+ + +	+ + +
Piriform cortex (Pir)	+ + + +	+ + + +
Prelimbic cortex (PrL)	+ + +	+ + +
Retrosplenial agranular cortex (RSA)	+ + +	+ + +
Retrosplenial granular cortex (RSG)	+ + +	+ + +
Somatosensory cortex, primary (S1)	+ +	+
Somatosensory cortex, secondary (S2)	+ +	+
Temporal association cortex (TeA)	+ +	+

3.2 Olfactory

Impressive MCH-1R mRNA signal was observed throughout the olfactory area (Table 3.2). The dorsal and ventral tenia tecta, indusium griseum, and the olfactory tubercle contained very strong signal. Strong signal was seen in the dorsal, lateral, medial, and ventral anterior olfactory nuclei, while only moderate signal was expressed in the glomerular layer of the olfactory bulb in the mouse (Figs. 3.2A-F, 3.3G, 3.6A-E).

Table 3.2: Relative Expression Densities of MCH-1R in the Olfactory

	Mouse	Rat
Anterior olfactory nucleus, dorsal (AOD)	+ + +	+ + +
Anterior olfactory nucleus, lateral (AOL)	+ + +	+ + +
Anterior olfactory nucleus, medial (AOM)	+ + +	+ + +
Anterior olfactory nucleus, ventral (AOV)	+ + +	+ + +
Olfactory bulb, glomerular layer (GI)	+ +	n/a
Olfactory tubercle (Tu)	+ + + +	+ + + +
Tenia tecta, dorsal (DTT)	+ + + +	+ + + +
Tenia tecta, ventral (VTT)	+ + + +	+ + + +
Indusium griseum (IG)	+ + + +	+ + + +

3.3 Basal Ganglia and Septum

The strongest signal that was observed in the basal ganglia and septum regions was found in the shell of the nucleus accumbens (Table 3.3). This very strong signal was expressed in both the mouse and rat brains, however, the nucleus accumbens core contained strong signal exclusively in the mouse (Figs. 3.2C,D, 3.6C,D, 3.9G-I). The caudate putamen also displayed a differential expression between the mouse and rat brain. The mouse expressed MCH-1R mRNA strongly throughout the entire caudate putamen (Figs. 3.2C-F, 3.3G-J). Conversely, the rat brain weakly expressed signal in the caudate putamen and the signal was isolated to its most rostra-medial aspect (Figs. 3.2C-F, 3.3G,H, 3.6C-F, 3.9D-F). Moderate expression was observed in the substantia nigra compacta as well as low expression in the lateral septal dorsal and septofimbrial nuclei (Figs. 3.2F, 3.6D,E). Moderate expression was also noted in the interstitial nucleus of the posterior limb of the anterior commissure in the mouse while the rat contained low expression in this area (Fig. 3.2F).

Table 3.3: Relative Expression Densities of MCH-1R in the Basal Ganglia

	Mouse	Rat
Accumbens nucleus, core (AcbC)	+ + +	+ + +
Accumbens nucleus, shell (AcbSh)	+ + + +	+ + + +
Caudate putamen (CPu)	+ + +	+
Interstitial nu. posterior limb ant. commissure, lateral (IPAC)	+ +	+
Substantia nigra, compact part (SNC)	+ +	+ +
Lateral septal nucleus, dorsal (LSD)	+	+
Septofimbrial nucleus (SFi)	+	+

3.4 Amygdala

Relatively low MCH-1R mRNA neuronal expression was observed throughout the amygdala (Table 3.4). The ventral and anterior basolateral amygdaloid, posterodorsal and posteroventral medial amygdaloid, and posteromedial cortical amygdaloid nuclei, along with the posterolateral bed nucleus of the stria terminalis displayed weak expression (Figs 3.3G-K, 3.6F, 3.7G-J). Weak expression was also seen in the anterior cortical amygdaloid nucleus in the mouse but contained moderate expression in the rat (Figs. 3.3I, 3.7G). Moderate signal was also noted in the posteromedial amygdalohippocampal area in the mouse and in the intercalated nuclei of the amygdala in both mouse and rat. (Figs. 3.2F, 3.3J,K, 3.7I,J) The densest signal was found in the posterolateral amygdaloid nucleus as well as the posteromedial amygdalohippocampal area in the rat (Figs 3.3J,K, 3.7G-J).

Table 3.4: Relative Expression Densities of MCH-1R in the Amygdala

	Mouse	Rat
Anterior cortical amygdaloid (ACo)	+	+ +
Amygdalohippocample area, postermedial (AHiPM)	+ +	+ + +
Basolateral amygdaloid n., anterior (BLA)	+	+
Basolateral amygdaloid n., ventral (BLV)	+	+
Bed nucleus of the stria terminalis, posterolateral (BSTMPL)	+	+
Intercalated nuclei of the anygdala (I)	+ +	+ +
Medial amygdaloid nucleus, posterodorsal (MePD)	+	+
Medial amygdaloid nucleus, posteroventral (MePV)	+	+
Posterolateral cortical amygdaloid n. (PLCo)	+ + +	+ + +
Posteromedial cortical amygdaloid n. (PMCo)	+	+

3.5 Hippocampal Formation

In the hippocampal formation, very strong hybridization expression was observed in the pyramidal cell layer of CA1, CA2, and in the fasciola cinereum (Figs 3.3I,J, 3.7H,I). A high number of positive cells were noted in the subiculum and in the pyramidal cell layer of CA3 and was given a strong rating (Figs. 3.3I,K,L, 3.7H,J,K). The septal hippocampal nucleus contained the weakest signal in the hippocampal region (Table 3.5, Figs. 3.2E, 3.6E).

Table 3.5: Relative Expression Densities of MCH-1R in the Hippocampal Formation

	Mouse	Rat
Ammon's horn, CA1	+ + + +	+ + + +
Ammon's horn, CA2	+ + + +	+ + + +
Ammon's horn, CA3	+ + +	+ + +
Fasciola cinereum (FC)	+ + + +	+ + + +
Septal hippocampal nucleus, (SHi)	+	+
Subiculum (S)	+ + +	+ + +

3.6 Thalamus and Hypothalamus

The majority of positive areas in the thalamus expressed weak to moderate MCH-1R mRNA levels (Table 3.6, 3.7). Low expression was observed in the central medial, central lateral, and paracentral thalamic nuclei in the mouse while having slightly stronger signal in the rat (Figs. 3.3H,I, 3.7G). Conversely, moderate expression was noted in the dorsal lateral geniculate, habenular, and paraventricular thalamic nuclei in the mouse while having only weak expression in the rat (Figs. 3.3H-J, 3.7G,H). Weakly hybridized neurons were also observed in the laterodorsal, anterior paraventricular, reunien, suprageniculate, and ventromedial thalamic nuclei as well as the subthalamic and peripeduncular nuclei (Figs 3.3H-K, 3.7G-K). The hypothalamus

contained only slightly higher hybridization expression than in the thalamus. The lateral mammillary nucleus contained the largest number of strongly stained neurons in the hypothalamus followed by the medial supramammillary nucleus and the medial mammillary nucleus (Figs. 3.3L, 3.7I,K). Moderate signal expression was also seen in the acuate and ventromedial hypothalamic nuclei, which are known to regulate feeding in mammals, as well as in the dorsal and ventral premammillary nuclei (Figs. 3.3J,K, 3.7G). In the mouse, moderate signal was noted in the supraoptic nucleus and the paraventricular hypothalamic nucleus, where as these areas contained weaker expression in the rat (Figs 3.3H,I). The rat brain displayed a low level expression in the medial preoptic area however this signal was not seen in the mouse (Fig. 3.6F, 3.9J-L). Both mouse and rat displayed low signal in the posterior region of the anterior hypothalamic area, the dorsalmedial hypothalamic nucleus as well as in the zona incerta (Figs. 3.3I-K, 3.7G-J).

Table 3.6: Relative Expression Densities of MCH-1R in the Thalamus

	Mouse	Rat
Central lateral thalamic nucleus, (CL)	+	+ +
Central medial thalamic nucleus, (CM)	+	+ +
Dorsal lateral geniculate nucleus (DLG)	+ +	+
Habenular nucleus (Hb)	++	+
Laterodorsal thalamic nucleus,	+	+
Paracentral thalamic nucleus (PC)	+	+ +
Paraventricular thalamic nucleus, anterior (PVA)	+	+
Paraventricular thalamic n. (PV)	+ +	+
Peripeduncular nucleus (PP)	+	+
Reunien thalamic nucleus (Re)	+	+
Subthalamic nucleus (STh)	+	+
Supragenicuiate thalamic nucleus (SG)	+	+
Ventromedial thalamic nucleus (VM)	+	+

Table 3.7: Relative Expression Densities of MCH-1R in the Hypothalamus

	Mouse	Rat
Anterior hypothalamic area, posterior (AHP)	+	+
Arcuate hypothalamic nucleus (Arc)	+ +	+ +
Dorsalmedial hypothalamic n. (DMH)	+	+
Lateral hypothalamus (LH)	+	+
Lateral mammillary nucleus (LM)	+ + +	+ + +
Supramammillary nucleus, medial (SuMM)	+ +	+ +
Medial mammillary nucleus, medial (MM)	+ +	+ +
Medial preoptic area (MPO)	-	+
Supraoptic nucleus (SO)	+ +	+
Paraventricular hypothalamic nucleus (PVN)	+ +	+
Premammillary nucleus, dorsal (PMD)	+ +	+ +
Premammillary nucleus, ventral (PMV)	+ +	+ +
Ventromedial hypothalamic nucleus (VMH)	+ +	+ +
Zona incerta (ZI)	+	+

3.7 Brainstem

The neuronal MCH-1R mRNA expression in the brainstem was found to be situated in punctate clusters of positive neurons residing in specific areas. Weak to moderate expression was observed in the serotonergic dorsal raphe, median raphe, and raphe magnus cell groups as well as the tegmental areas including the ventral tegmental, lateraldorsal tegmental areas and the reticulotegmental nucleus of the pons (Figs. 3.4M-P, 3.7K-I). The pontine areas including the pontine nucleus and the oral and caudal pontine reticular nuclei contained moderately hybridized neurons (Figs. 3.4N-Q, 3.9L-N). Strong neuronal staining was evaluated in the motor trigeminal nucleus and in the ventral cochlear anterior nucleus (Figs. 3.4P,Q, 3.8M,N). Throughout the brainstem, many neurons with moderate level of expression were observed in the gigantocellular reticular nucleus, the principal sensory trigemimal dorsomedial nucleus, the red parvicellular nucleus, and the parvicellular reticular alpha nucleus (Figs. 3.4M-R, 3.5S,

3.7K,L, 3.8M). The lowest MCH-1R mRNA expressing cells in the brainstem were found in the Darkschewitsch nucleus, oculomotor nucleus, and the superior paraolivary and inferior olive nuclei (Figs. 3.4M,N,R, 3.5T, 3.7L, 3.8N,P). Three areas in the brainstem displayed a differential MCH-1R expression between the mouse and rat. The noradrenergic locus coeruleus, as well as the optic nerve layer of the superior colliculus, contain neurons expressed MCH-1R mRNA very strongly in the rat brain but not in the mouse (Figs. 3.7K,L, 3.8N, 3.9M-R). Conversely, strong expression in the lateral parabrachial nucleus was observed in the mouse but not in the rat brain (Table 3.8, Figs. 3.4R, 3.10P-R).

Table 3.8: Relative Expression Densities of MCH-1R in the Brainstem

	Mouse	Rat
Darkschewitsch nucleus (DK)	+	+
Dorsal raphe nucleus (DR)	+ +	+ +
Gigantocellular reticular n. (Gi)	+ +	+ +
Inferior olive (IO)	+	+
Lateral parabrachial nucleus (LPB)	+ + +	-
Laterodorsal tegmental n. (LDTg)	+	+ +
Locus coeruleus (LC)	-	+ + + +
Oculomotor nucleus (3N)	+	+
Optic nerve layer of the superior colliculus (Op)	-	+ + + +
Median raphe nucleus (MnR)	+ +	+
Motor trigeminal nucleus (Mo5)	+ + +	+ + +
Parvicellular reticular nucleus, alpha (PCRtA)	+ +	+ +
Pontine nucleus (Pn)	+ +	+
Pontine reticular nucleus, caudal (PnC)	+ +	+ +
Pontine reticular nucleus, oral (PnO)	+ +	+ +
Principal sensory trigeminal nucleus, dorsomedial (Pr5DM)	+ +	+ +
Raphe magnus nucleus (RMg)	+	+ +
Red nucleus, parvicellular (RPC)	+ +	+ +
Reticulotegmental nucleus, pons (RtTg)	+ +	+
Superior paraolivary nucleus (SPO)	+	+ +

Table 3.8: *Continued*

Ventral cochlear nucleus, anterior (VCA)	+ + +	+ + +
Ventral tegmental area (VTA)	+ +	+ +

Overall, the majority of brain areas expressing MCH-1R mRNA correspond well between these two mammalian species. However, it was discovered that a small number of these regions differentially displayed the MCH-1 receptor. In the mouse, MCH-1R expression was observed in the core region of the accumbens, throughout the caudate putamen, and in the lateral parabrachial nucleus in which these expressions were absent or greatly reduced in the rat brain. The accumbens receives dopaminergic input from the ventral tegmental area along the mesolimbic pathway and is considered the pleasure center of the brain (Kandel et al. 2000). It is thought that this area increases dopamine in the brain as a reward (finding a good supply of food for example) (Kandel et al. 2000). The caudate putamen also received dopaminergic inputs from the ventral tegmental area as well as the substantia nigra and is involved in movement and learning (Kandel et al. 2000). Finally, the lateral parabrachial nucleus is important in taste response behavior and relays this information to the cortex (Kandel et al. 2000). All of these sites seem to be involved in food intake and consequently could explain any differences in feeding behavior between mice and rats. In contrast, the rat contained signal in the medial preoptic nucleus, the claustrum and dorsal endopiriform nuclei, as well as strong signal in the optic nerve layer of the superior colliculus and locus coeruleus which was not displayed in the mouse. The medial preoptic area controls reproductive behaviors as well as body temperature and blood pressure and does not

seem to be directly involved in food intake or foraging (Kandel et al. 2000). However, the claustrum and dorsal endopiriform nuclei are believed to be areas that coordinate and interpret sensory input like visual cues and emotional states which could be important in feeding behaviors (Crick et al., 2005, Kandel et al. 2000). The optic nerve layer of the superior colliculus is important in visually guided eye movements and relays input directly from the retina to the cortex (Kandel et al. 2000). Also, the locus coeruleus controls vigilance states and behavior responses to unexpected environmental stimuli. It is obvious that both the optic nerve layer of the superior colliculus and the locus coeruleus are important in visually detecting a possible food source while keeping the animal awake to collect or capture and ingest the food. This differential expression between mice and rats was unexpected and suggests the function of the MCH ligand may be slightly different in these two species.

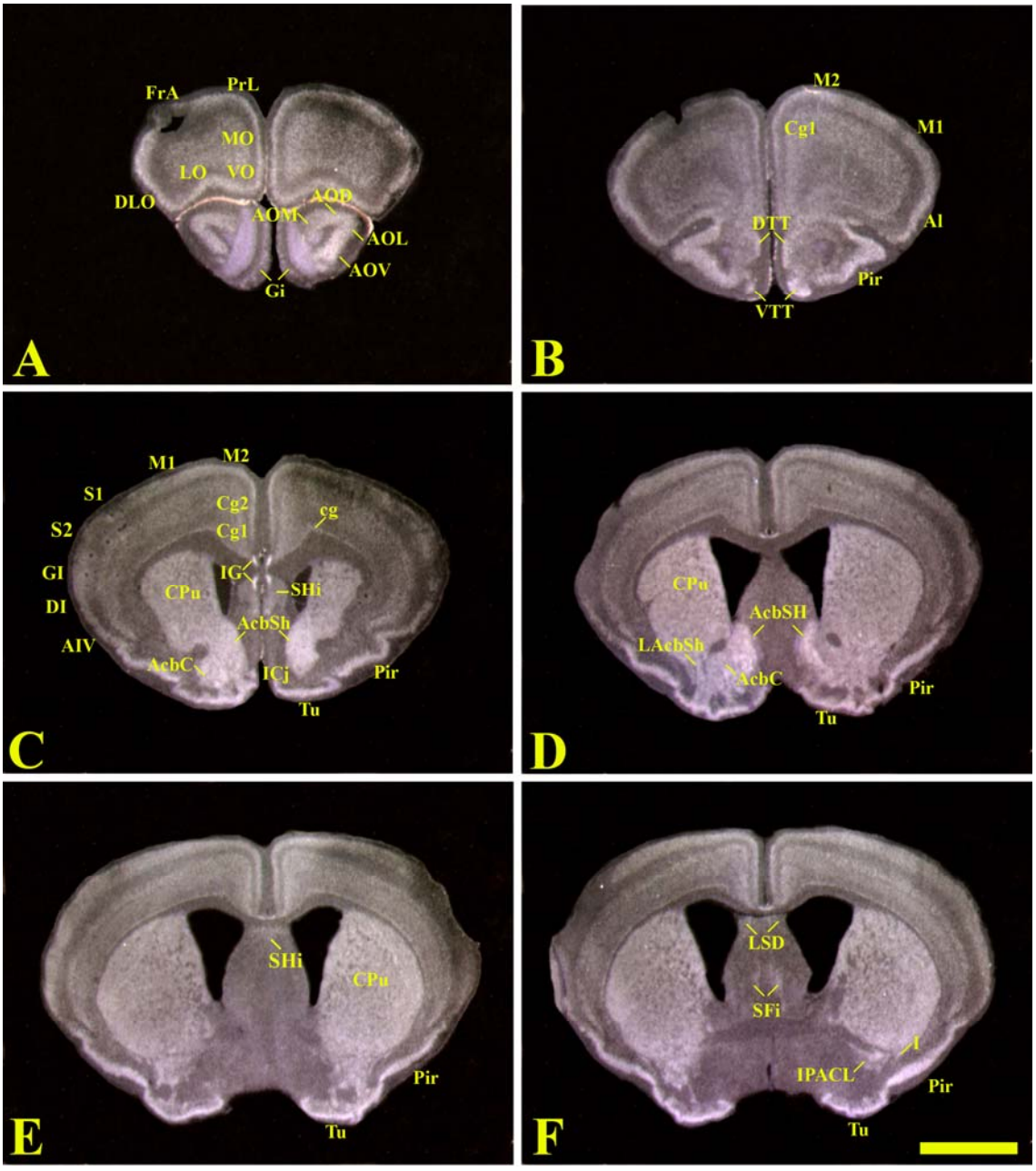

Figure 3.2: MCH-1R mRNA expression in the mouse forebrain
((A,B,C,D,E,F) Sequential sections through the forebrain.)
(Please see tables for an explanation of the abbreviations. Scale bar = 2mm)

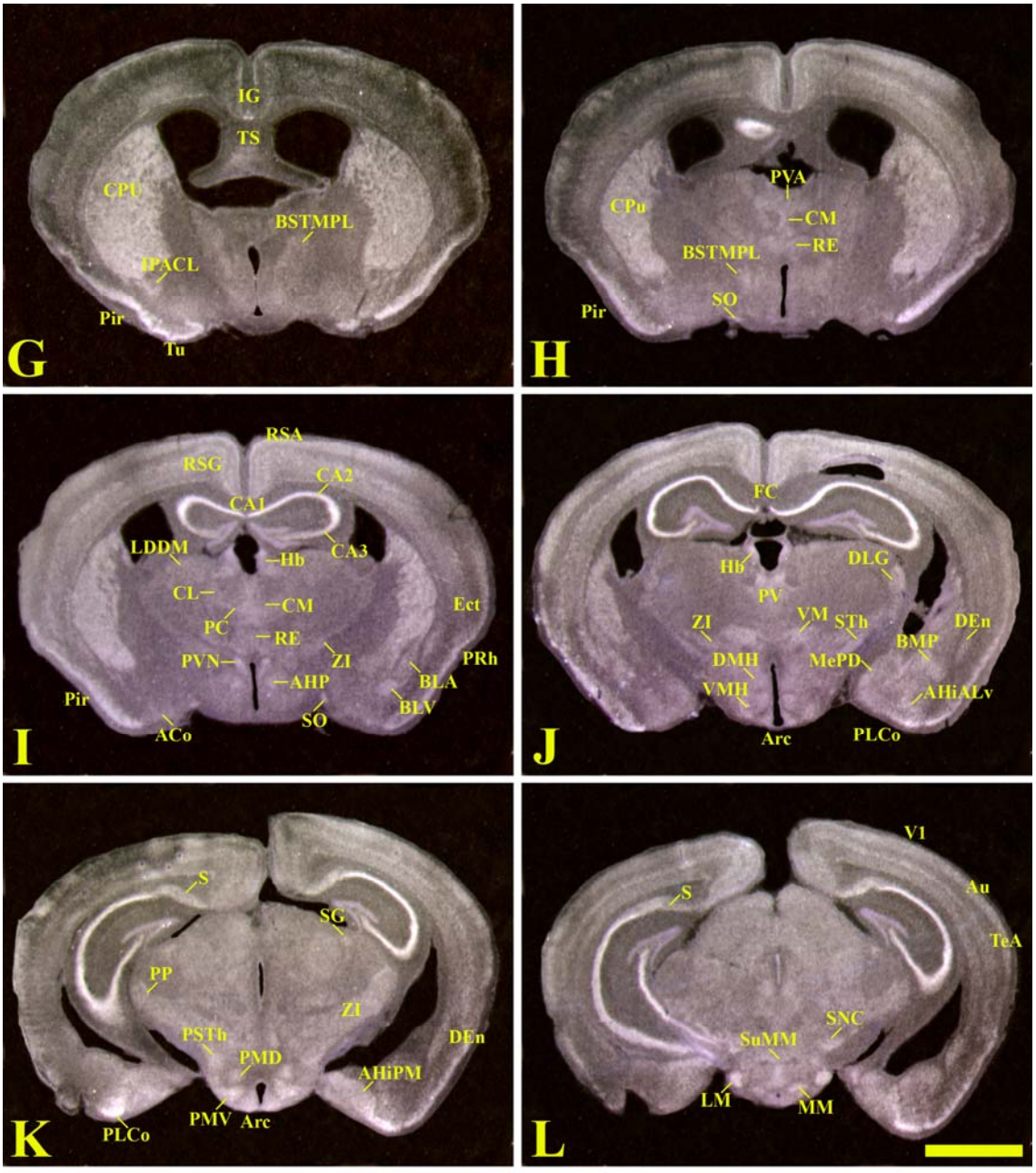

Figure 3.3: MCH-1R mRNA expression in the mouse midbrain
((G,H,I,J,K,L) Sequential sections through the midbrain.)
(Please see tables for an explanation of the abbreviations. Scale bar = 2mm)

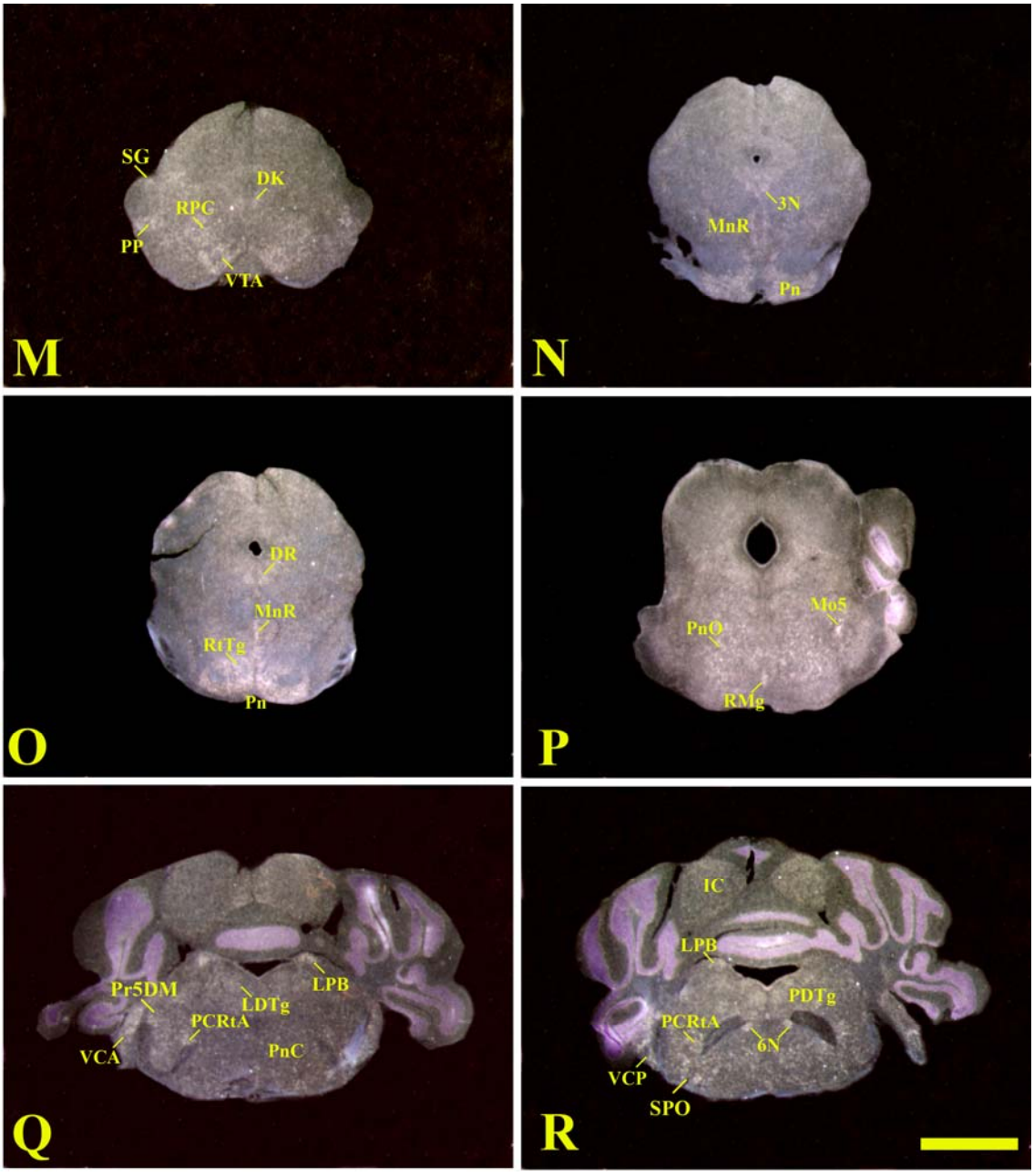

Figure 3.4: MCH-1R mRNA expression in the mouse hindbrain
((M,N,O,P,Q,R) Sequential sections through the hindbrain.)
(Please see tables for an explanation of the abbreviations. Scale bar = 2mm)

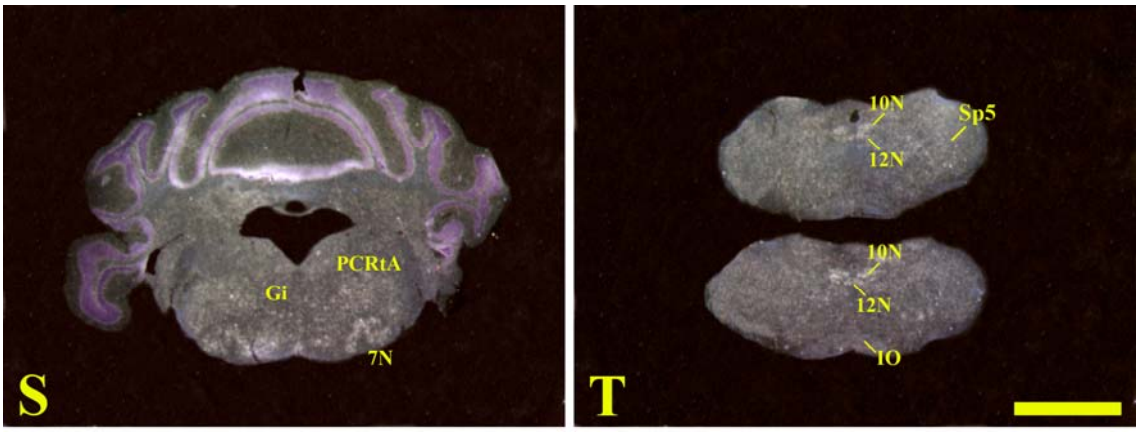

Figure 3.5: MCH-1R mRNA expression in the mouse hindbrain
((S,T) Sequential sections through the hindbrain.)
(Please see tables for an explanation of the abbreviations. Scale bar = 2mm)

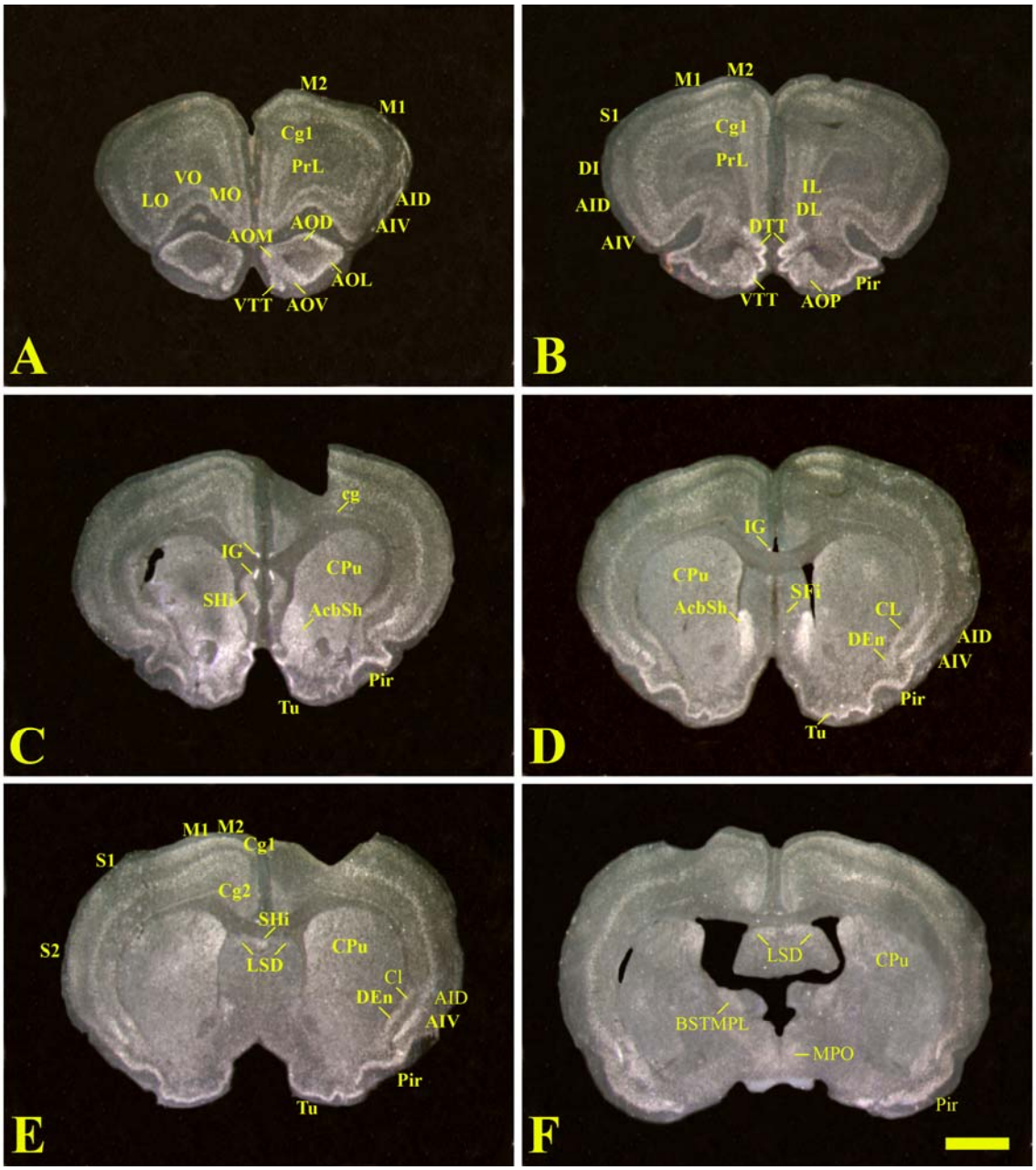

Figure 3.6: MCH-1R mRNA expression in the rat forebrain
((A,B,C,D,E,F) Sequential sections through the forebrain.)
(Please see tables for an explanation of the abbreviations. Scale bar = 2mm)

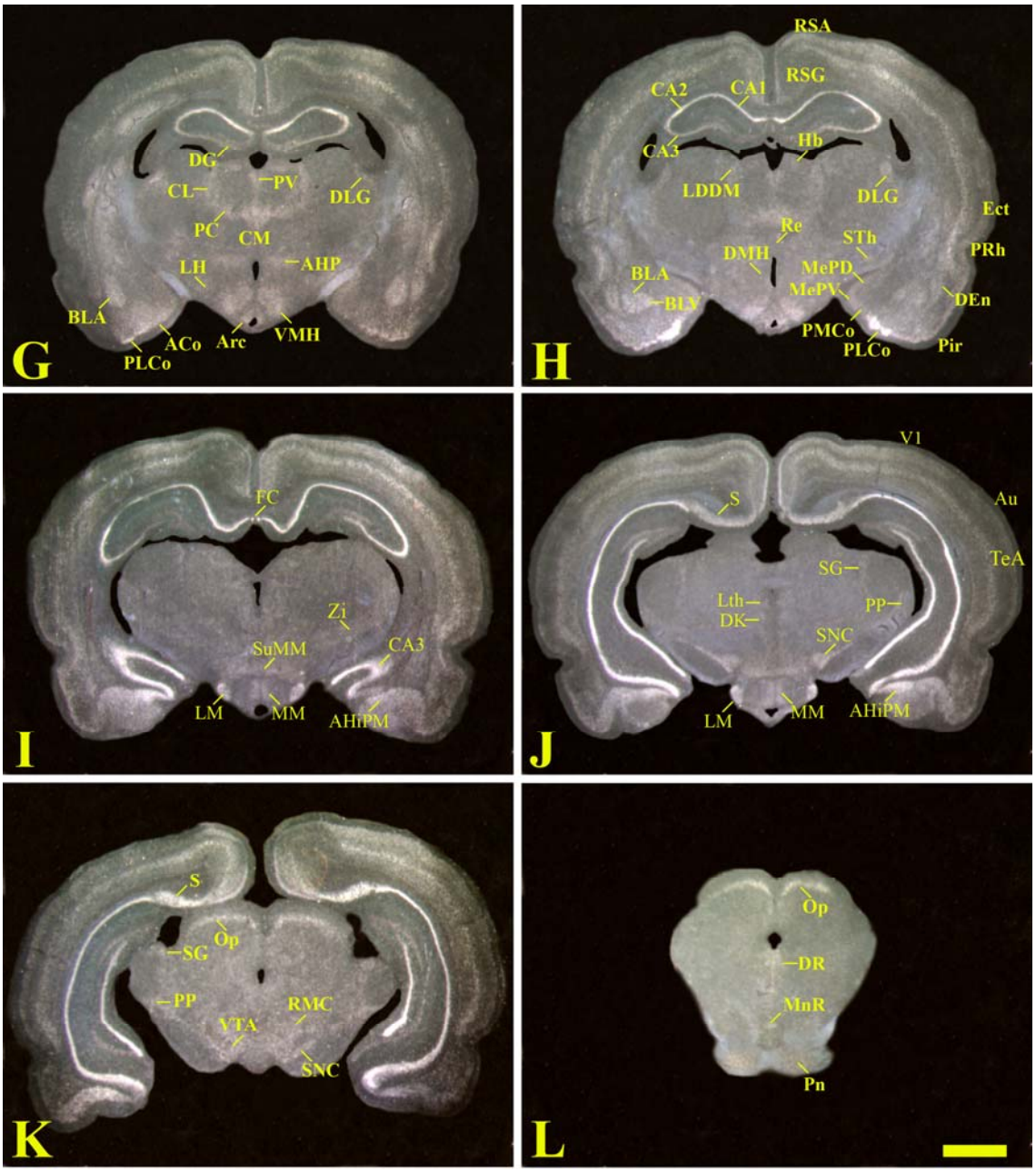

Figure 3.7: MCH-1R mRNA expression in the rat midbrain
((G,H,I,J,K,L) Sequential sections through the midbrain.)
(Please see tables for an explanation of the abbreviations. Scale bar = 2mm)

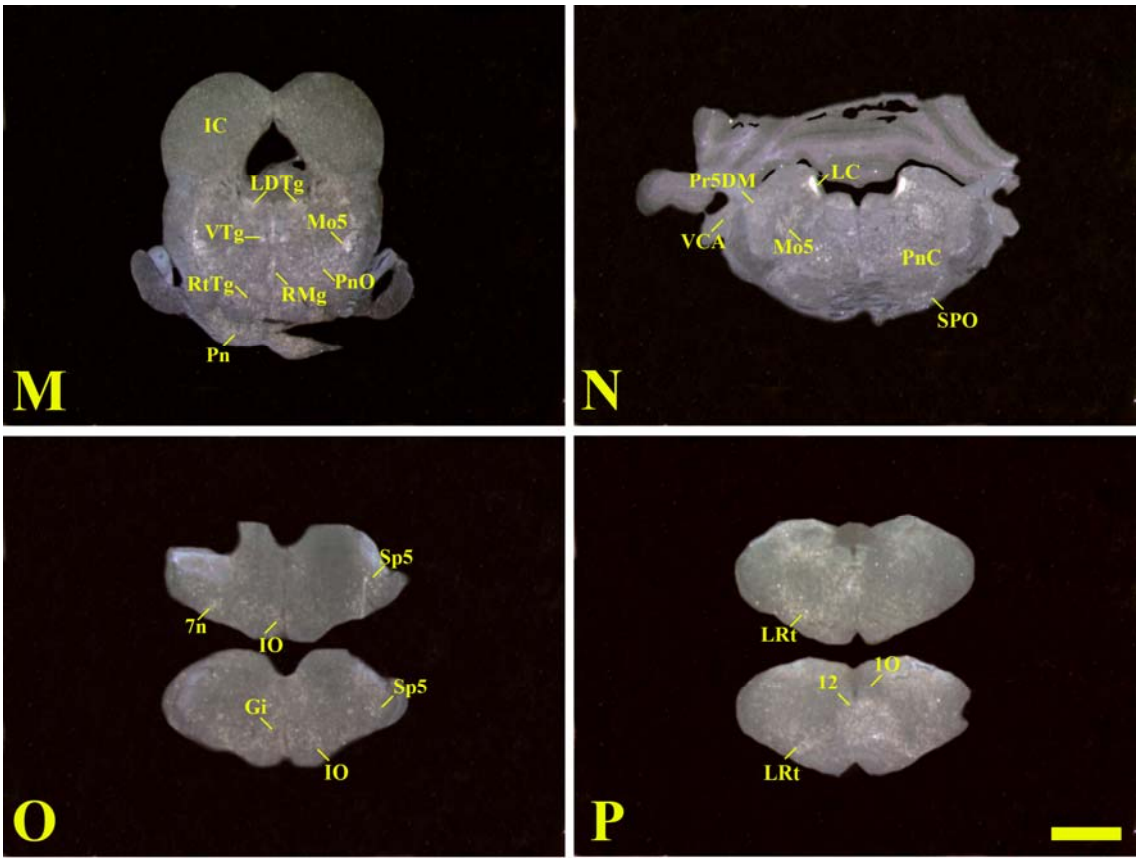

Figure 3.8: MCH-1R mRNA expression in the rat hindbrain
((M,N,O,P) Sequential sections through the hindbrain.)
(Please see tables for an explanation of the abbreviations. Scale bar = 2mm)

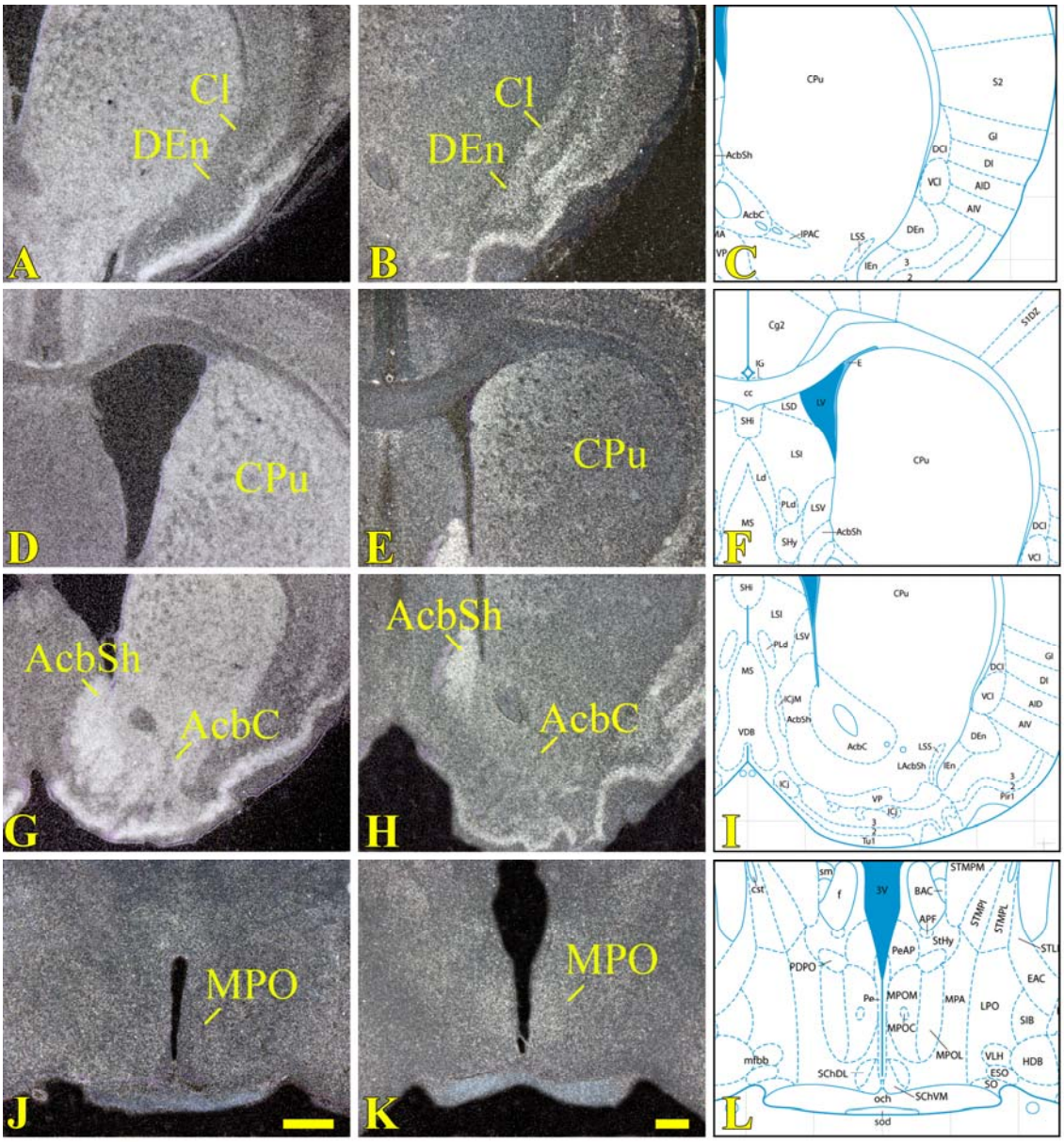

Figure 3.9: Brain regions differentially expressing MCH-1R mRNA ((A,D,G,J)Mouse brain, (B,E,H,K) Rat brain, (C,F,I,L) Diagrams from Paxinos and Watson, Scale bars = 0.5mm)

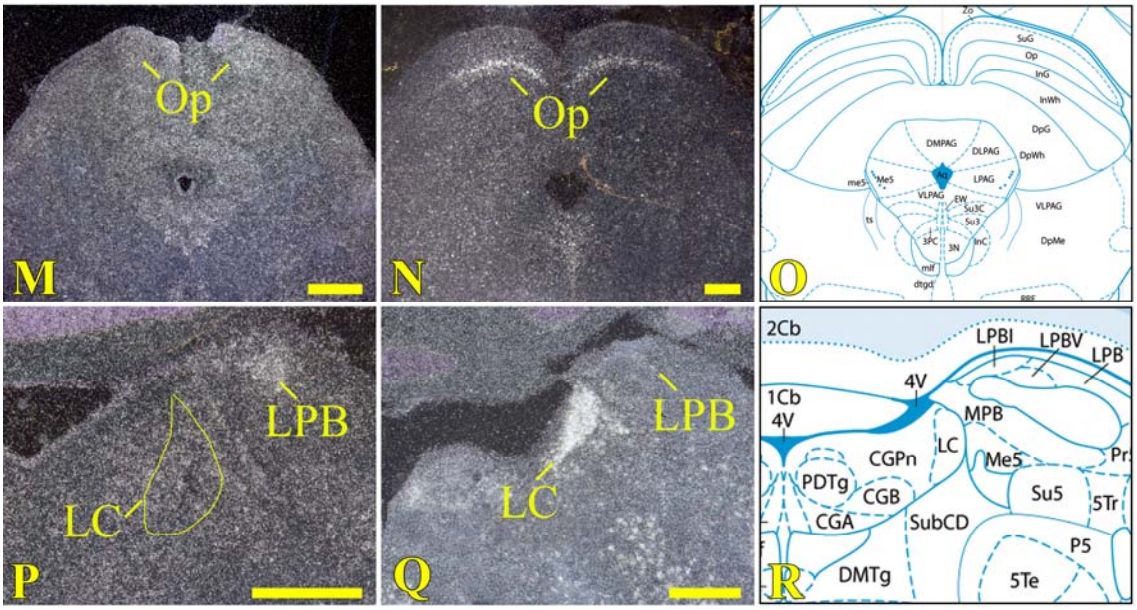

Figure 3.10: Brain regions differentially expressing MCH-1R mRNA ((M,P)Mouse brain, (N,Q) Rat brain, (O,R) Diagrams from Paxinos and Watson, Scale bars = 0.5mm)

CHAPTER 4

DISCUSSION

Both MCH and MCH-1R are important in regulating food intake in rodents and MCH and MCH-1R null mice are significantly leaner than their wild-type littermates. The chronic infusion of MCH-1R antagonists in the brains of rodents also reduces body weight, thus making it a possible site for pharmacological control of obesity. Interestingly, publications describing the distribution of the MCH-1R have been performed using only rat brain. However, all the genetically manipulated animals and many of the behavior studies have been performed using mice. Therefore, we have performed radioactive *in situ* hybridization specifically in mouse brain and have noted a difference in MCH-1R expression between rats and mice.

Mice and rats are two different species of mammals and may have different neurochemistry. Thus, mice and rats can exhibit different behaviors when presented with the same stimuli and/or pharmacological reagents. Because both of these animals are used extensively in research, it has been easy to consider them equivalent and assume that they express all proteins in the same manner. For example, the lack of MCH-1R expression in the noradrenergic locus coeruleus in mice may contribute to a difference in how MCH influences sleep/wake cycles or how the animals explore novel environments.

However, it is also important to consider the technique used to determine the brain areas expressing the MCH-1 receptor. Radioactive *in situ* hybridization only labels neurons that are currently transcribing the RNA that codes for the production of the MCH-1R protein. Thus, this technique can only reveal that a neuron is currently producing a specific protein but not the functional site of the protein. In other words, it will only label the area where the mRNA is residing, which in most cases is in the cell body, not where the protein is being transported. The protein could be transported down an axon or dendrite away from the cell body. Therefore, it is possible that the areas differentially expressing MCH-1R in mice and rats could still be influenced by MCH. For example, when MCH is injected directly into brains of mice it stimulates feeding. However, MCH-1R is a Gi-coupled protein which decreases neuronal activity of the neuron in which it is expressed. Consequently, it is possible that MCH-1R is expressed in, and directly inhibits, the neurons that suppress appetite. Alternatively, it may act presynaptically to inhibit an inhibitory projection to areas that stimulate feeding. Currently, it is not known how the MCH-1R elicits its inhibitory effect. Therefore, immunohistochemical studies using antibodies specific for MCH-1R and MCH need to be performed to answer this question.

Antagonists that block the activity of the MCH-1R have been shown to decrease body weight in rodents as well as elicit antidepressant and anxiolytic effects. Therefore, MCH-1R has become a potential pharmacological site for the control of obesity, depression and anxiety. Because of the differences in MCH-1R expression in the brains of rodents, it is important to determine the MCH-1R expression pattern in the brains of

humans. Using an animal model that expresses MCH-1R most like humans would more accurately predict the effect of a trial drug in humans and thus circumvent possible adverse effects in humans that were not observed in the animal model used.

In summary, we have compared the areas expressing MCH-1R mRNA in the brains of mice and rats. This comparison study revealed that most of the positive nuclei evaluated were represented in both rodent models and that these areas displayed similar expression intensities. However, a subset of nuclei were found to express this receptor differentially and many of these areas could be involved in the control of feeding. Detailed immunohistochemical studies are now needed to elucidate the functional sites of the MCH-1R. These studies would provide valuable information about possible pre-synaptic interactions as well as data about the type of neurons expressing the MCH-1R.

REFERENCES

Abbott C.R., Kennedy A.R., Wren A.M., Rossi M., Murphy K.G., Seal L.J., Todd J.F., Ghatei M.A., Small C.J., Bloom S.R. (2003) Identification of hypothalamic nuclei involved in the orexigenic effect of melanin-concentrating hormone. Endocrinology, 144:3943–3949.

Bachner D., Kreienkamp H.J., Weise C., Buck F., Richter D. (1999) Identification of melanin concentrating hormone (MCH) as the natural ligand for the orphan somatostatin-like receptor 1 (SLC-1). FEBS Letters, 457:522–524.

Bittencourt J.C., Presse F., Arias C., Peto C., Vaughan J., Nahon J.L., Vale W., Sawchenko P.E. **(**1992) The melanin-concentrating hormone system of the rat brain: an immuno- and hybridization histochemical characterization. Journal of Comparative Neurology, 319:218–245.

Borowsky, B., Durkin, M.M., Ogozalek, K., Rarzabadi M.R., DeLeon, J., Heurich, R., Lichtblau, H., Shaposhnik, A., Daniewska, I., Blackburn, T.P., Branchek, T.H., Gerald, C., Vaysse, P.J., Forray, C. (2002) Antidepressant, anxiolytic and anorectic effects of a melanin-concentrating hormone-1 receptor antagonist. Nature Medicine, 8:825-830.

Chambers J., Ames R.S., Bergsma D., Muir A., Fitzgerald L.R., Hervieu G., Dytko G.M., Foley J.J., Martin J., Liu W.S., Park J., Ellis C., Ganguly S., Konchar S., Cluderray J., Leslie R., Wilson S., Sarau H.M. (1999) Melanin-concentrating hormone

is the cognate ligand for the orphan G protein coupled receptor SLC-1. Nature, 400:261–265.

Chen, Y., Hu, C., Hsu, C.-K., Zhang, Q., Bi, C., Asnicar, M., Hsiung, H.M., Fox, N., Slieker, L.J., Yang, D.D., Heiman, M.L., Shi, Y., (2002) Targeted disruption of the melanin-concentrating hormone receptor-1 results in hyperphagia and resistance to diet-induced obesity. Endocrinology, 143, 2469– 2477.

Crick, F.C., Koch, C. (2005) What is the function of the claustrum? Philosophical Transactions of the Royal Society B, 360, 1271-1279.

Hill, J., Duckworth, M., Murdock, P., Rennie, G., Sabido-David, C., Ames, R.S., Szekeres, P., Wilson, S., Bergsma, D.J., Gloger, I.S., Levy, D.S., Chambers, J.K., Muir, A.I. (2001) Molecular cloning and functional characterization of MCH2, a novel human MCH receptor. Journal of Biological Chemistry, 276, 20125-20129.

Lembo P.M.C., Grazzini E., Cao J., Hubatsch D.A., Pelletier M., Hoffert C., St-Onge S., Pou C., Labrecque J., Groblewski T., O'Donnell D., Payza K., Ahmad S., Walker P. (1999) The receptor for the orexigenic peptide melanin-concentrating hormone is a G-protein-coupled receptor. Nature Cell Biology, 1:267–271.

Ito M., Gomori A., Ishihara A., Oda Z., Mashiko S., Matsushita H., Yumoto M., Ito M., Sano H., Tokita S., Moriya M., Iwaasa H., Kanatani A. (2003) Characterization of MCH-mediated obesity in mice. American Journal of Physiology Endocrinology and Metabolism, 284:E940–E945.

Kandel, E.R., Schwartz, J.H., Jessell, T.M., (2000) Principles of neural science. New York, N.Y: McGraw-Hill Inc.

Kawauchi, H., Kawazoe, I., Tsubokawa, M., Kishida, M. & Baker, B.I. (1983) Characterization of melanin concentrating hormone in chum salmon pituitaries. Nature, 305, 321-323.

Kolakowski L.F., Jung B.P., Nguyen T., Jonson M.P., Lynch K.R., Heng H.H.Q., Geroge S.R., O'Dowd B.F. (1996) Characterization of a human gene related to genes encoding somatostatin receptors. FEBS Letters,398:255–258.

Ludwig D.S., Tritos N.A., Mastaitis J.W., Kulkarni R., Kokkotou E., Elmquist J., Lowell B., Flier J.S., Maratos-Flier E. **(**2001) Melanin-concentrating hormone overexpression in transgenic mice leads to obesity and insulin resistance. Journal of Clinical Investigations, 107:379–386.

Marsh, D.J., Weingarth, D.T., Novi, D.E., Chen, H.Y., Trumbauer, M.E., Chen, A.S., Guan, X.-M., Jiang, M.M., Feng, Y., Camacho, R.E., Shen, Z., Frazier, E.G., Yu, H., Metzger, J.M., Kuca, S.J., Shearman, L.P., Gopal-Truter, S., MacNeil, D.J., Strack, A.M., MacIntyre, D.E., Van der Ploeg, L.H.T., Qian, S., (2002) Melanin-concentrating hormone 1 receptor-deficient mice are lean, hyperactive, and hyperphagic and have altered metabolism. Proceedings of the National Academy of Science U.S.A., 99, 3240–3245.

Mashiko, S., Ishihara, A., Gomori, A., Moriya, R., Ito, M., Iwaasa, H., Matsuda, M., Feng, F., Shen, Z., Marsh, D.J., Bednarek, M.A., MacNeil, D.J., Kanatani A. (2005) Antiobesity effect of a melanin-concentrating hormone 1 receptor antagonist in diet-induced obese mice. Endocrinology, 146:3080-3086.

Paxinos, G., Franklin, K.B.J. (2004) The mouse brain in stereotaxic coordinates. Burlington, MA: Elsevier Academic Press.

Paxinos, G., Watso, W. (2005) The rat brain in stereotaxic coordinates. Burlington, MA: Elsevier Academic Press.

Qu D., Ludwig D.S., Gammeltoft S., Piper M., Pelleymounter M.A., Cullen M.J., Mathes W.F., Przypek R., Kanarek R., Maratos-Flier E. **(**1996) A role for melanin-concentrating hormone in the central regulation of feeding behavior. Nature, 380:243–247.

Sailer, A.W., Zeng, Z., McDonald, T.P., Pan, J., Pong, S.S., Feighner, S.D., Tan, C.P., Kukami, T., Iwassa, H., Hreniuk, D.L., Morin, N.R., Sadowski, S.S., Ito, M., Bansal, A., Ky, B., Figueroa, D.J., Jiang, Q., Austin, C.P., MacNeil, D.J., Ishihara, A., Ihara, M., Kanatani, A., Van der Ploeg, L.H.T., Howard, A.D., Liu, Q. (2001) Identification and characterization of a second melanin-concentrating hormone receptor, MCH-2R. Proceedings of the National Academy of Science U.S.A., 98,7564-7569.

Saito Y., Nothacker H-P., Wang Z., Lin S.H.S., Leslie F., Civelli O. (1999) Molecular characterization of the melanin-concentrating hormone receptor. Nature, 400:265–269.

Shearman, L.P., Camacho, R.E., Stribling, D.S., Zhou, D., Bednarek, M.A., Hreniuk, D.L., Feighner, S.D., Tan C.P., Howard, A.D., Van der Ploeg, L.H.T., MacIntyre, D.E., Hickey, G.J., Strack A.M. (2003) Chronic MCH-1 receptor modulation alters appetite, body weight and adiposity in rats. European Journal of Pharmacology, 475:37-47.

Shimada M., Tritos N.A., Lowell B.B., Flier J.S., Maratos-Flier E. (1998) Mice lacking melanin-concentrating hormone are hypophagic and lean. Nature, 396:670–674.

Shimomura Y., Mori M., Sugo T., Ishibashi Y., Abe M., Kurokawa T., Onda H., Nishimura O., Sumino Y., Fujino M. (1999) Isolation and identification of melanin-concentrating hormone as the endogenous ligand of the SLC-1 receptor. Biochemistry Biophysics Communications, 261:622–626.

Tan, C.P., Sano, H., Iwassa, H., Pan, J., Sailer, A.W., Hreniuk, D.L., Feighner, S.D., Palyha, O.C., Pong, S.S., Figueroa, D.J., Austin, C.P., Jiang, M.M., Yu, H., Ito, J., Ito, M., Guan, X.M., MacNeil, D.J., Kanatani, A., Van der Ploeg, L.H., Howard, A.D. (2002) Melanin-concentrating hormone receptor subtypes 1 and 2 species-specific gene expression. Genomics, 79, 785-792.

Teitelbaum, P., Cheng, M.F., Rozin, P. (1969) Stages of recovery and development of lateral hypothalamic control of food and water intake. Annuals New York Academy of Science, 157, 849-860.

Vaughan, J.M., Fisher, W., Hoeger, C., River, J. & Vale, W. (1989). Characterisation of melanin-concentrating hormone from rat hypothalamus. Endocrinology, 125, 1660-1665.

Wang, S., Dehan, J., O'Neil, K., Weig, B., Fried, S., Laz, T., Bayne, M., Gustafson, E., Hawes, B.E. (2001) Identification and pharmacological characterization of a novel human melanin-concentrating hormone receptor, MCH-R2. Journal of Biological Chemistry, 276, 34640-34670.

BIOGRAPHICAL INFORMATION

Clay Williams entered the University of Texas at Arlington as a freshman in the fall semester of 1989 pursuing a degree in engineering. However, after completing an introduction course in biology, he quickly changed his major to Biological Sciences. During his time as an undergraduate, he had the privilege to work in the laboratory of Dr. Howard Arnott. Here, Clay enjoyed working on a wide variety of projects and was exposed to microphotography, light and electron microscopy, and histology. After graduating with a Bachelors of Science in Biology in the Spring of 1995, he started working for the Howard Hughes Medical Institute in the laboratory of Dr. Masashi Yanagisawa at the University of Texas Southwestern Medical Center in Dallas. Clay continued to take classes at the University of Texas at Arlington as a degreed undergrad and finally entered the graduate program in 2005. Currently, Clay continues to work with Dr. Yanagisawa as a Research Specialist utilizing his strong background in microscopy, photography, and histology on a daily basis. He has been involved in many exciting scientific discoveries and his photography has been published in journals, science magazines, and textbooks. This summer he is planning to obtain ASCP Histotechnologist and Immunhistochemistry certifications and would like to continue his education at UT Arlington in the Ph.D. program.